JET–P(97)05

High Performance Joint European Torus (JET) Plasmas for Deuterium-Tritium Operation with the Mk II Divertor

T T C Jones and the JET Team.

JET Joint Undertaking, Abingdon, Oxfordshire, OX14 3EA, UK.

Preprint of a paper accepted for publication in
the proceedings of the 38th Meeting of the APS Division of Plasma Physics
(Denver, USA, 11-15 November 1996)

February 1997

ABSTRACT

Planned experiments in the Joint European Torus [Plasma Physics and Controlled Fusion Research (Proc 13th Int Conf Washington, 1990) (International Atomic Energy Agency, Vienna) **1** 27 (1991)] (JET) with Deuterium-Tritium (D-T) plasmas require high fusion performance for α-particle heating studies and for investigation of isotope dependence in conditions relevant to the International Thermonuclear Experimental Reactor [Plasma Physics and Controlled Fusion **37** A19 (1995)]. In deuterium plasmas, the highest neutron rates have been obtained in the hot-ion High-confinement mode (H-mode) which is ultimately limited by Magnetohydrodynamic (MHD) phenomena when the pressure gradient approaches ideal ballooning and kink stability limits in the vicinity of the edge transport barrier. Results are reported confirming the MkII divertor's increased closure and pumping in this regime, progress in understanding the MHD-related termination is discussed, and the use of Ion Cyclotron Resonance Heating (ICRH) in combination with high power neutral beams to increase the neutron yield is described. In separate experiments internal transport barriers have been established through careful programming of the current ramp and heating waveforms, and neutron emission comparable with the best hot-ion modes achieved. Steady-state H-mode discharges exhibiting Edge Localised Modes (ELMs) in reactor-like configurations and conditions have been demonstrated, including cases in which relevant dimensionless parameter values are preserved, ready also for testing in D-T.

PACS numbers: 52.55.F, 52.50, 52.35P, 52.65

* See Appendix A for JET Team authors.

I. INTRODUCTION

A. Joint European Torus (JET) programme objectives

The JET[1] programme to the end of 1999 has two main scientific objectives: (i) to make essential contributions to the development and demonstration of a viable divertor concept for the International Thermonuclear Experimental Reactor (ITER) device[2]; and (ii) carry out experiments using Deuterium-Tritium (D-T) plasmas in an ITER-like configuration which will provide a firm basis for the D-T operation of ITER. The first phase of D-T experiments, denoted DTE1, is scheduled to start in early 1997 and the broad objectives include the study of α-particle heating effects and isotope dependence of High-confinement mode (H-mode) enhancement and power threshold in reactor-like plasmas. This paper discusses recent progress on the high performance plasma regimes, operated in the presently installed MkIIA divertor configuration[3], from which the DTE1 scenarios will be selected. Three regimes are discussed, the hot-ion H-mode displaying periods free of Edge Localised Modes (ELMs); the Internal Transport Barrier (ITB) with optimised central shear; and the steady-state ELMy H-mode with plasma parameters and configurations

relevant to ITER. These high performance studies represent only part of the present JET campaign; the development and demonstration of a viable divertor concept for ITER represents the other main branch of the programme[3] which has involved the staged implementation of divertors with successively optimised geometry and power handling capability and includes model validation against the experimental results.

B. Modifications to the JET device for the 1996 campaign

The MkIIA divertor installed for the 1996-7 campaign offers an increased degree of closure against neutrals created at the target plate escaping into the main chamber and a larger conductance to the cryo-pump, as well as a larger wetted target area compared with MkI, (see comparison in Figure 1). A number of other modifications were also made which have increased JET's operating flexibility. The Neutral Beam (NB) shinethrough and drift-duct protection have been further upgraded which has permitted an extension of the NB operating space to even lower plasma density and plasma current, and has had a direct impact on the ability to establish the ITB mode. The outboard poloidal limiter structures have been slightly modified to avoid shadowing the antennae of the Ion Cyclotron Resonance Heating (ICRH) system in shaped configurations necessary for long ELM-free periods in hot-ion H-modes, and this regime has been successfully developed to utilise supplementary ICRH in combination with the predominant NB heating to boost fusion performance. In parallel with these modifications and the operational programme, the technical preparations for DTE1 have continued and are nearing completion. The closed-circuit facility for tritium supply and recovery is presently in an advanced state of commissioning, together with new tritium-compatible distribution networks for the NB injectors and torus gas fuelling. Since completing the experiments reported in the present work the gas leakage conductance paths between the divertor and main chamber have been substantially closed off, and the inner wall has been extensively clad with graphite tiles in order to reduce the exposed metallic surface area of this region from ≈50% to ≈10%.

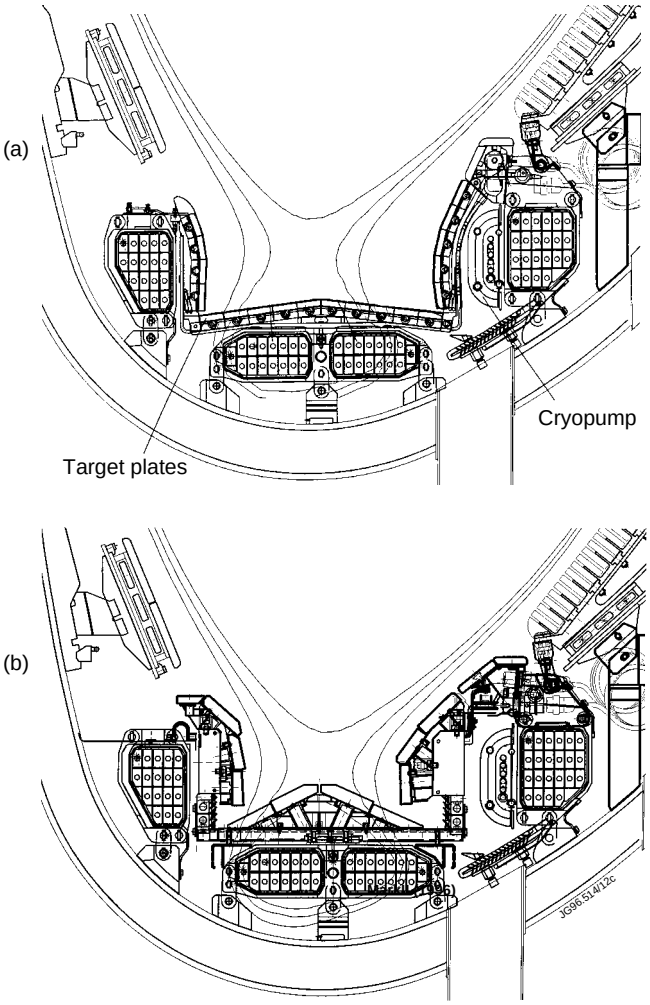

Figure 1: Poloidal cross-section of the Mk I (top) and Mk IIA (bottom) JET pumped divertors

Technical preparations are complete for a further in-vessel modification of the divertor to a 'gas-box' configuration, denoted MkIIGB, which will be undertaken using fully remote-handling techniques, in summer 1997, shortly following DTE1.

C. Outline of progress in the high performance regimes

During the period of the 1996 campaign to date, the available power from the NB injectors has been restricted to about 17MW due to technical problems with some of the NB sources, compared with the installed maximum of >20MW in deuterium which was achieved in the previous campaign. This has so far prevented a full exploitation of the MkIIA divertor, and maximum Deuterium-Deuterium (D-D) neutron emission and projected D-T fusion amplification factor Q in 1996 has not yet exceeded the best results in the MkI configuration obtained in 1995; full NB power will however be restored before DTE1. Despite this limitation good progress has been made in all high performance modes, especially in the development of the ITB. The hot-ion H-mode results are discussed in section II. Similar D-D neutron yields as in the MkI campaign have been obtained when compared at the same NB power, whilst with combined heating (NB+ICRH) 80% of the previous highest neutron rate has been obtained. Most of the features of the hot-ion mode in the previous campaign have been observed with the MkIIA divertor, in particular the variety of Magnetohydrodynamic (MHD) related termination events which lead to degradation in confinement and an irreversible loss of performance. Progress in identifying the MHD instabilities responsible is discussed; the mechanism by which the MHD events cause the loss of confinement is, however, still unclear. Low recycling conditions are a pre-requisite for good hot-ion mode performance, as is well known from results obtained in the Preliminary Tritium Experiment[4] (PTE) and subsequently in the MkI divertor experiments. The superior particle control properties of the MkIIA divertor have allowed this aspect to be studied further, with lower recycling levels achieved. Substantial progress has been made on the ability to model the behaviour of hot-ion H-modes predictively, and it is shown how the present models are able simultaneously to describe successfully both the confinement and stability properties of these plasmas which helps to provide a coherent interpretation of the roles of particle recycling and MHD stability as well providing insight into the transport properties of the regime. In section III the development of ITB in JET through the use of carefully tailored current ramps and heating waveforms is described, and the properties of these discharges is discussed. Whilst evidence for ITB has been observed in previous JET experiments, such as the Pellet Enhanced Plasma (PEP) + H-mode[5], these new results, which are at high combined heating power, achieve very high neutron emission rates almost identical with the best combined heating hot-ion H-mode, maintained for more than an energy confinement time and represent a possible alternative to the hot-ion H-mode for DTE1 high-fusion yield. ELMy H-mode results, where genuine steady-state ITER-relevant conditions have been obtained, are presented in section IV. Experiments have been performed in which the dimensionless parameters of normalised larmor radius

ρ^* ($\propto T^{1/2}/Ba$), collisionality ν^* ($\propto nT/B^2$) and β are independently varied, with ν^* and β ranging up to their ITER values; this provides a firmer basis for assessing the validity of scaling laws used for ITER, such as ITERH93-P[6].

II. HOT-ION H-MODE

A. General features

It was clearly established during the MkI divertor campaign that the necessary conditions for obtaining a long ELM-free period include low recycling[7] and shaping[8] of the equilibrium to provide sufficient edge shear through triangularity. The same technique was immediately successful in the MkIIA campaign; Figure 2 shows the time traces for a typical NB heated hot-ion mode. The density pumps out following X-point formation to $\approx 1\times10^{19}m^{-3}$ when full power heating is applied. Low density, with moderate T_e ($\approx$12keV) and hence decoupled electron and ion temperatures contributes to the favourable confinement properties in the presence of strong ion-heating by NB[9], together with the dominant effect of the H-mode edge transport barrier. The stored energy increases almost linearly, until termination by a simultaneous sawtooth and giant ELM, in this case after the beam power was reduced. The saturation of ion-temperature as the density rises is a characteristic behaviour. Figure 3 shows the D-D neutron rate plotted against heating power for NB-only cases, comparing MkI and MkIIA divertor campaigns. The highest

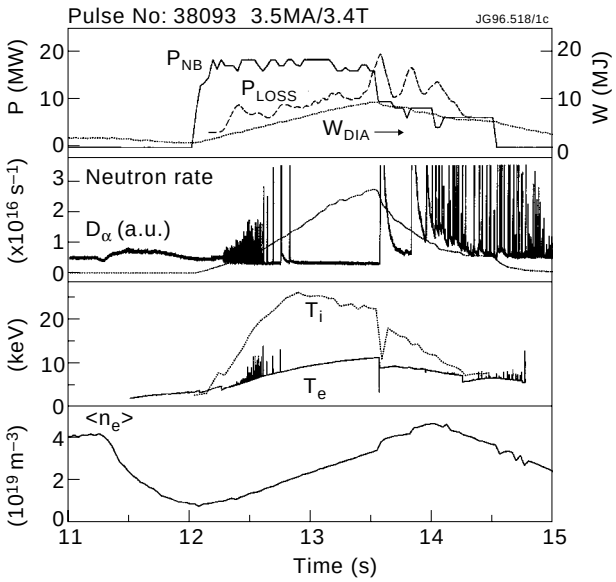

Figure 2: Typical time traces of a hot-ion H-mode plasma showing neutral beam power P_{NB}, plasma loss power P_{LOSS}, diamagnetic stored energy W_{DIA}, D-D neutron emission, D_α signal, central ion and electron temperatures T_i and T_e and volume averaged density $<n_e>$

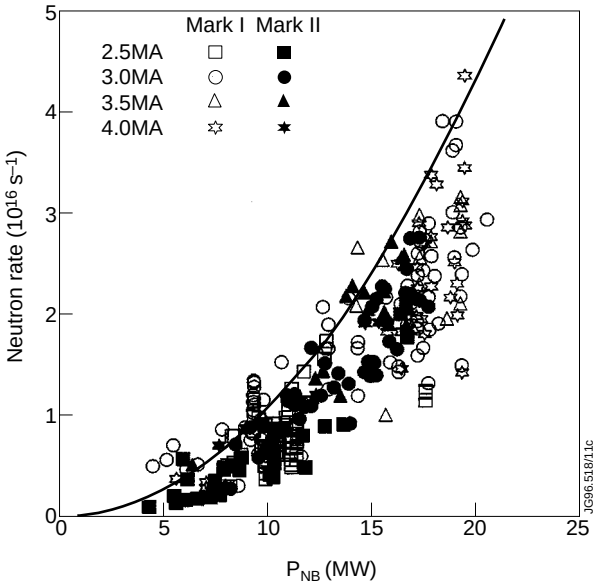

Figure 3: Neutron rate plotted against total neutral beam power in hot-ion H-mode discharges. Open symbols refer to Mk I and closed symbols refer to Mk IIA divertor. The symbol shapes indicate plasma currents as shown.

yields are obtained in the plasma current range 3-4MA at 3.4T, with $3 < q_{95} < 4$, triangularity $\delta > 0.3$ and edge shear $S_{95} > 3.5$. More highly shaped configurations with $\delta > 0.6$ and $S_{95} > 4$ have also been investigated but the plasma current was limited to 2.5MA due to machine operating limits. The solid line in the figure is an approximate representation of the upper bound of the data, drawn proportional to P_{NB}^2; a similar dependence is observed for the two campaigns. There no sign of saturation of the P_{NB}^2 dependence of the attainable yield, despite the limit being set by MHD-triggered loss of confinement and the termination tending to occur earlier as the power is raised. This is explained by the increase in the rate of rise of central density and temperature at higher power, sustained until the power flux and pressure gradient build up at the edge sufficiently to trigger the termination event (usually an ELM or 'outer mode', section C), transiently leading to higher stored energy and more peaked profiles.

B. Effect of increased divertor closure

A useful figure of merit which characterises the particle recycling level in an ELM-free H-mode is the ratio of the rate of increase in the plasma electron content compared with the neutral beam fuelling source; in the MkI divertor this ratio was generally greater than 1. Values of this figure close to or even less than 1 have been obtained in the MkIIA divertor campaign, consistent with the increased closure and particle removal rate. The data in Figure 4 summarise the particle balance in terms of plasma content, wall inventory and pumped particles for hot-ion H-modes under similar NB heating as a function of number of gas-fuelled atoms. The principal difference is the greater particle removal by the cryo-pump in MkIIA, as predicted, due to the development of higher neutral gas pressures and larger pumping conductance[3]. In the MkI campaign favourable low recycling conditions were obtained only without gas fuelling following X-point formation and after extensive vessel and target conditioning[7,8], whilst for MkIIA the optimum performance was obtained with a modest gas bleed before and during the heating and there

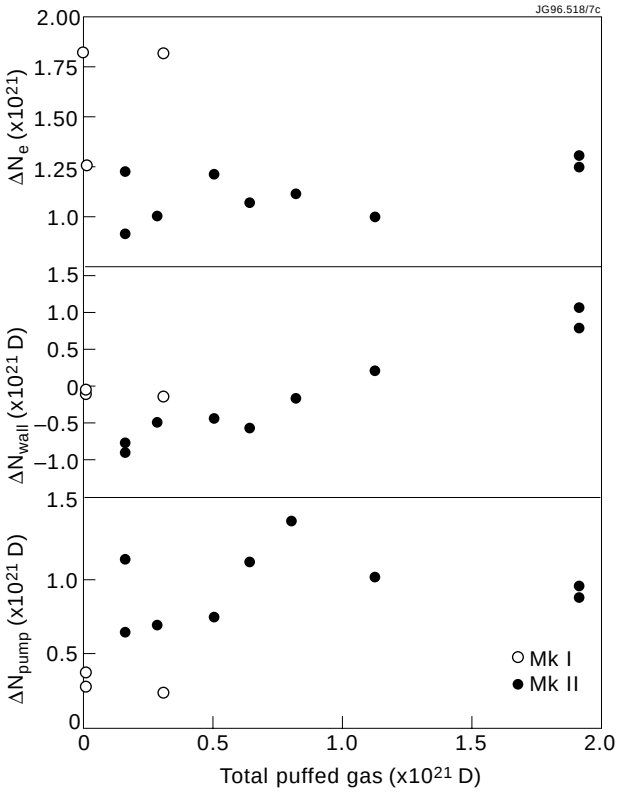

Figure 4: Particle balance over the first second of neutral beam heating in ELM-free hot-ion H-modes. The changes in the particle contents of the plasma, wall surfaces, and cryo-pump inventory are plotted as a function of total gas-fuelled particles over the same interval. The NB heating is 17MW in all cases which corresponds to a particle input of 1.4×10^{21} s^{-1}.

was no need for special conditioning other than routine overnight beryllium evaporation. There is evidence that at the extreme of low recycling without gas fuelling in MkIIA, the target density can pump out too much, resulting in excessive NB shinethrough losses and higher Z_{eff}. Figure 4 indicates that the walls become depleted under strong divertor pumping at low gas fuelling rate, implying they represent a particle source of significant strength compared with the external sources. Experiments[10] in which the inner-wall surfaces of the vessel were selectively loaded with hydrogen showed that these surfaces are important contributors to the wall sources during ELM-free periods. These results support the decision to install more extensive graphite cladding on the inner-wall surfaces in order to reduce hydrogenic outgassing and desorption (induced by charge-exchanged neutrals) from exposed inconel.

C. MHD termination events

1. Classification and characteristics of termination events

High performance hot-ion H modes are affected by a variety of MHD instabilities which limit the achieved performance, by triggering a serious loss of confinement. A similar variety of phenomena have been observed in the present campaign as those previously reported[11], namely central MHD events (including sawteeth), giant (or type I) ELMs, and 'outer-modes' (OMs) located within the radial region r/a $\gtrapprox$ 0.8. Sawteeth are especially damaging at $\beta_N \gtrapprox 1.5$ when they often couple to giant ELMs or OMs. The distribution of the occurrence of these phenomena is also quite similar in the two campaigns; the majority of terminations involve either a giant ELM or OM. The outer mode exhibits both global and local characteristics. The stored energy and neutron rate saturate or decline; for this reason the OM phenomenon is also termed 'slow rollover'; the divertor D_α signal rises during low frequency (≈10kHz) magnetic activity of structure n=1-4, m=3-12. From Electron Cyclotron Emission (ECE) and Soft X-Ray (SXR) measurements, the activity appears to be close to the q=3 surface. This is illustrated by the ECE data in Figure 5 where the effect of the OM can be seen as a prompt degradation in transport at all

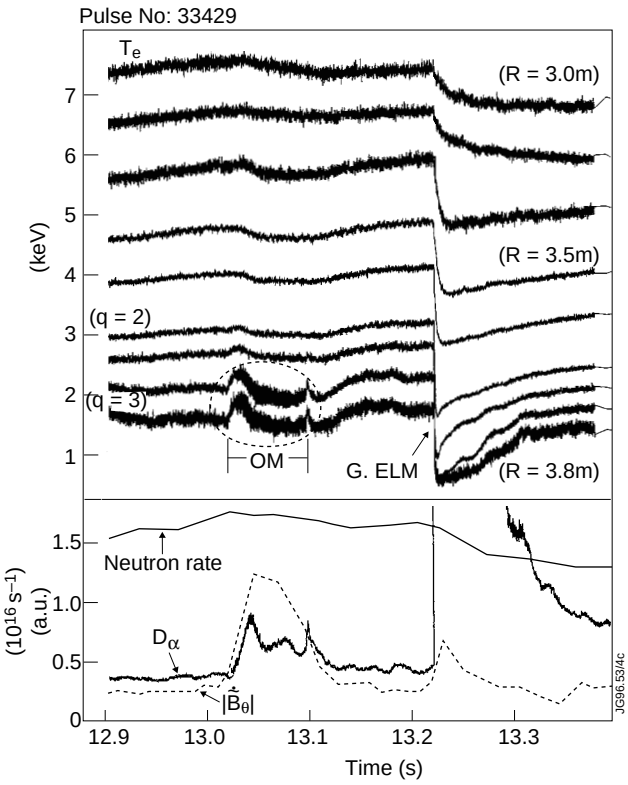

Figure 5: Time traces for a plasma whose performance is limited by an outer mode (OM) and a giant ELM (G.ELM). A range of localised electron temperature traces are shown from the axis to the edge, together with the neutron rate, D_α and magnetic pick-up coil signals

radial locations. The effect of the ELM is similar, but, in addition, due to the large number of ionisations at the plasma edge as evidenced by the D_α spike, a cold wave diffusively propagates from the edge inwards. From detailed analysis of SXR emissivity profiles, the OM activity has been identified as an ideal kink, by comparing the relative phases of measured SXR signals with those expected from the computed distortions of the SXR emissivity profile in the presence of the kink eigenmodes. By the same technique, it has been possible to discount the presence of tearing modes as a cause of the OM. The mechanism for the loss of confinement is not understood, but appears to imply a non-local dependence of transport. The confinement can sometimes recover after an early OM decays. One factor in the usual irreversibility of the loss of fusion performance is the difficulty to separate the ion and electron temperatures following the collapse when the density is high; this is particularly true following giant ELMs and late OMs.

2. MHD stability analysis

Analysis of the pressure gradients close to the plasma edge indicates that the ideal ballooning limit always appears to set the upper bound to the experimental values. In consequence of the significant neoclassical bootstrap current density associated with such pressure gradients, the edge can also become unstable to ideal kink modes. Hot-ion H-modes approach the limits of both ideal ballooning and kink stability and so from the theoretical viewpoint both classes of MHD mode would appear to play a role in the termination. The identification of the OM as an ideal kink close to the plasma edge is supported by MHD stability analysis of discharges exhibiting OMs. Further evidence is provided by the observation that negative current ramps of -0.2 to -0.3 MA s^{-1} can delay the OM onset. Ideal kink growth rate contours in the space of normalised edge current density and pressure gradient for a particular discharge are plotted in Figure 6 and the trajectory describing the time evolution of this discharge, based on the measured data, is shown, marking the time of an early OM onset when the trajectory is moving further into the kink-unstable domain. Termination by a giant ELM eventually occurs at the time when the ballooning limit is reached. The edge pressure gradient in some other discharges without OM can however remain at the ballooning limit for several 100ms before a giant ELM occurs. So far there is no direct conclusive experimental evidence to confirm the existence of ballooning modes when the edge pressure has saturated at the ballooning limit, although very

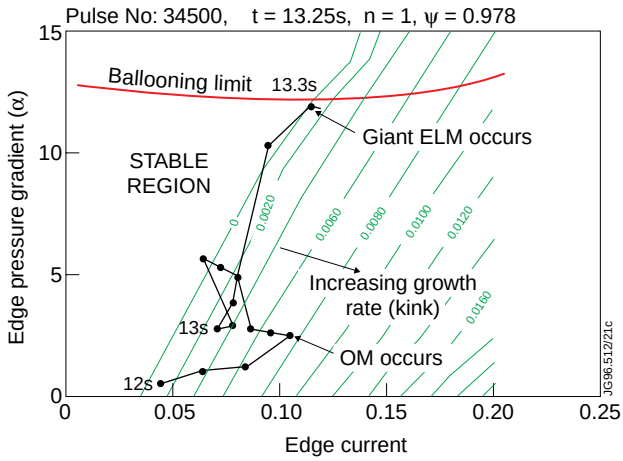

Figure 6: Edge MHD stability diagram of normalised presuure gradient (= $2\mu_0 Rq^2 p'/B_T^2$) versus normalised edge current (= J_{edge}/J_0). The lines to the right of the stable region are contours of the ideal kink growth rate. The trajectory of a pulse which exhibited outer modes and ELMs is shown.

recent fast magnetic pick-up data suggest the presence of modes with n > 5 and larger amplitude on the outboard side, reminiscent of ballooning. These characteristics suggest that neither ballooning nor ideal kink modes alone are sufficient to cause a giant ELM. Reaching the ballooning limit in combination with some other factor, possibly simultaneous proximity to the kink unstable region, appears to be necessary.

D. Predictive transport model

A neoclassical transport model for the edge transport barrier has been found to describe well many features of the JET hot-ion ELM-free H-mode, and has been incorporated into the time-dependent 11/2-dimensional predictive transport codes JETTO[12] and PRETOR[13]. A new code has also been developed in which JETTO has been linked to the Scrape-Off Layer (SOL) code EDGE2D/NIMBUS[14] with continuity of plasma quantities and fluxes imposed at the interface, located inside the separatrix surface. Core transport is described using a summation of non-local Bohm, local gyro-Bohm and ion neoclassical terms. The form of the transport coefficients is the same as in reference[12]. Transport at the edge is modelled assuming that within a layer of thickness Δ located just inside the separatrix, heat and particle diffusivities are related as follows:

$$D \approx \chi_e \approx \chi_i \approx \chi_i^{neo} \qquad (1)$$

where χ_i^{neo} is the neoclassical ion thermal diffusivity. The thickness Δ is taken to be of the order one ion banana-orbit width, i.e.

$$D \approx \varepsilon^{1/2} \cdot \rho_{\theta i} \qquad (2)$$

where ε is the inverse aspect ratio and $\rho_{\theta i}$ is the poloidal ion larmor radius. By making detailed measurements of the edge ion and electron temperature profiles the assumption defined by equation (2) has been tested. Figure 7(a) shows typical edge profile data taken during an ELM-free phase; the width Δ for many discharges at different plasma currents does approximately follow the $T^{1/2}$ dependence implied by (2) but the observed poloidal field dependence is weaker, Figure 7(b). A consequence of the neoclassical barrier described by equation (1) is that the heat flux through the barrier at low collisionality is independent of ion temperature[15] with:

$$q_{heat} \propto n^2 Z_{eff} \qquad (3)$$

In ELM-free H-mode simulations, following the application of heating the edge transport barrier is activated and the temperature-independent edge heat flux implied by equation (3) is then the main factor responsible for a near-linear rise of stored energy similar to the experimental observations. The non-local Bohm part of the core transport responds to the development of edge temperature pedestal which, in turn, causes a reduction in core transport; this combination of core and barrier transport models quantitatively reproduces the evolution of experimental

profiles and global quantities such as D-D neutron emission remarkably well. High-current hot-ion H-modes and their low-current analogues are both satisfactorily modelled without changing any model parameters except the global recycling coefficient which is always adjusted throughout the simulation such that the plasma electron content follows the experimentally observed evolution. In particular, the low-current analogue discharges develop more peaked pressure profiles, and therefore higher normalised β, due to the relative scaling of the edge and core transport and this is predicted satisfactorily by the codes despite the result expressed Figure 7(b) which does not fully support the poloidal field dependence of the barrier thickness. The edge barrier model also gives insight into the role of recycling in confinement and stability of the hot-ion H-mode. Equation (3) links confinement quality with recycling through the edge density; main-chamber recycling which penetrates across the separatrix is expected to be especially deleterious in this respect. The $T^{1/2}$ dependence of the edge pressure scale length, Δ, implies that there is a maximum limiting edge density in order to remain below a given constant ∇p, e.g. as set by ballooning at constant edge shear and poloidal field. The modelled ∇p(a) is close to both the ideal ballooning and kink limits, as observed experimentally. If the time of the termination is defined by reaching the edge ballooning limit, its appearance is satisfactorily predicted, provided only that the recycling coefficient is adjusted to match the experimental density rise.

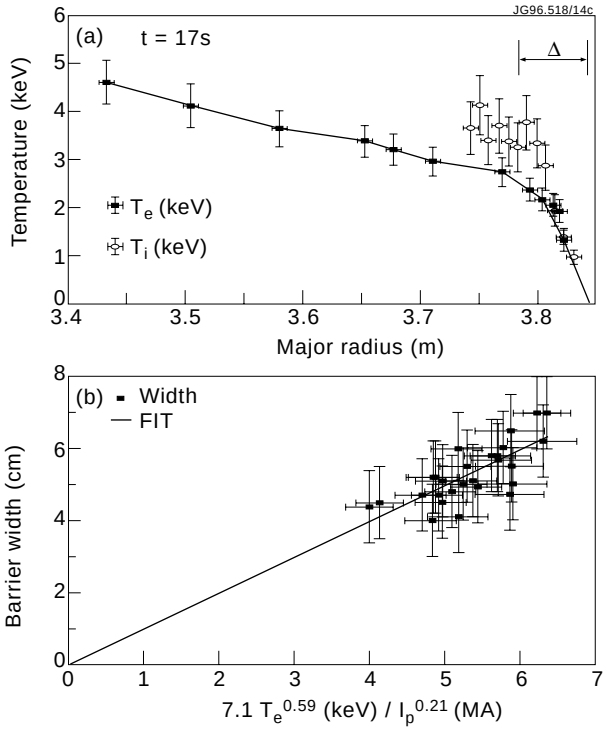

Figure 7: (a) Ion and electron temperature profiles for pulse 37444 (2.6MA/2.54T) from which the transport barrier width Δ is determined and (b) Δ plotted against fitted dependence on temperature and plasma current for hot-ion H-mode plasmas

E. Combined ICRH and NB heated hot-ion H-mode

Up to 9.5MW of hydrogen minority (H-minority) ICRH has successfully been combined with high power NB heating in the hot-ion H-mode achieving a substantial increase in D-D neutron emission. The discharge illustrated in Figure 8 reached the highest D-D neutron rate for the MkIIA configuration to date. With ICRH the rate of rise of neutron emission is significantly faster, but the termination generally comes earlier; sawtooth activity is also more abundant but can be ameliorated by the use of a double H-minority resonance in order to broaden the heating profile. Computations with the PION[16] code show that approximately 30% of the rf power is delivered to the plasma ions via the low-energy components of the H-minority and 2nd harmonic

rf accelerated D beam ion distributions, and direct 2nd harmonic damping on the thermal ions; the reduced ion-electron equilibration due to higher T_e also contributes to a more favourable ion power balance. The D-D neutron rate from high energy (>200keV) accelerated D^+ is computed to be <15% of the total, and can be further minimised through the use of multiple resonance techniques and by optimising the H-minority fraction for ion heating. By such optimisation the combined heating scenario can be further developed for D-T operation, although the translation of D-D performance to D-T projection is not as straightforward as the NB-only cases.

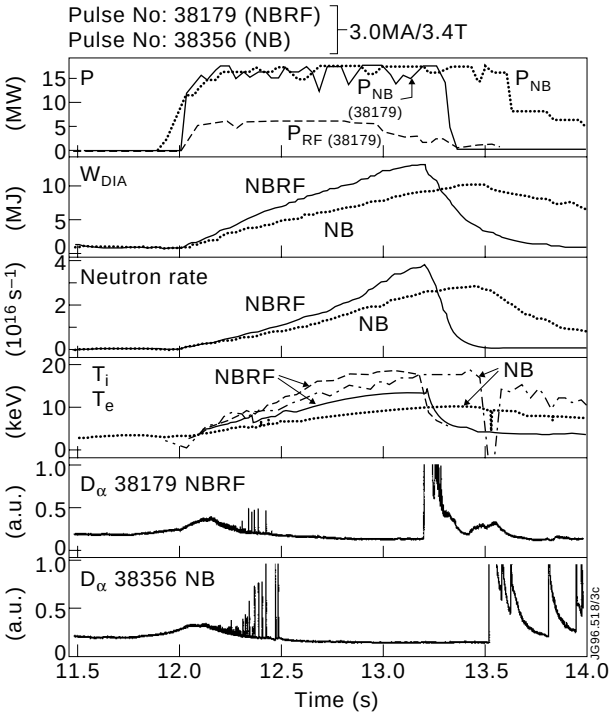

Figure 8: Time traces for hot-ion H-modes comparing NB-only (discharge #38356) and combined heating (denoted NBRF, discharge #38179). The traces shown are for the heating powers P_{NB} and P_{RF}, diamagnetic plasma stored energy W_{DIA}, neutron emission, central ion and electron temperatures and D_α intensity.

III. OPTIMISED CURRENT PROFILE AND INTERNAL TRANSPORT BARRIER FORMATION

A. Current profile control and performance enhancement

A number of previous experiments in JET have exploited some form of current profile modification for improved confinement. The PEP+H-mode[5] produced high fusion triple product and Q_{DD} values by the formation of ITB associated with reversed shear in the plasma core due to modification of the current profile as a result of deeply penetrating pellet injection. The high bootstrap current, high β_p mode[17] had substantially enhanced confinement, and active current profile control using Lower Hybrid Current Drive (LHCD) has been used successfully to raise the axial q >1 prior to formation of the hot-ion H-mode, thus eliminating sawteeth during the ELM-free phase and improving the initial neutron yield[18]; these discharges tended however to limit due to early ELM and OM onset which may have been attributable to a reduction in the internal inductance and edge shear. By taking advantage of the evolving current profile during the current rise and applying heating in such a way as to help preserve a favourable transient q profile, substantially enhanced confinement has been obtained within a significant proportion of the plasma volume in several devices[19-20], due to ITB formation, giving rise to potentially

significant fusion performance improvement. In the previous MkI divertor campaign, ITB was seen during electron heating by Lower Hybrid (LH) waves during a fast current ramp, but attempts to use NB heating were unsuccessful at that time. The technique has now been applied with considerable success in the JET MkIIA divertor campaign using high power combined NB + ICRH, and has demonstrated its potential as the basis of a possible candidate for high fusion power production in JET. This has been facilitated in part due to the reduction in the minimum density required for NB injection due to the technical improvements referred to in section I, giving the freedom to tailor the timing of the heating waveform to the evolving current profile whilst the density is still low.

B. Conditions for establishing ITB with combined NB+ICRH

A low triangularity discharge configuration capable of relatively fast initial current ramp-up of $\geq$ 0.5 MA s^{-1} was used for the majority of the experiments, the highest current ramp which avoids MHD activity and anomalous current penetration being adopted. Without additional heating sawteeth appear at about 2s after the plasma current has reached the flat-top value of 3MA. When high power heating is applied before the onset of sawteeth, ITB forms at a radius depending on the timing; early heating results in ITB formation at small radius which then moves radially outward and terminates disruptively. Such a case is illustrated in Figure 9(a), where the existence of the ITB is evidenced by the narrow region of steep ion temperature gradient. When MHD is present during the current rise there is evidence of significant current profile rearrangement from the observed change in internal inductance (l_i) and reduction in central q value leading to earlier disruptive termination. The effect of the ITB is also observed on the electron temperature profile, and, to a lesser extent, on the electron density profile. With early ITB formation the transport remains in the Low-confinement regime (L-mode) outside the ITB, right out to the plasma edge; this type of discharge is usually subject to fast rotating n=1 MHD mode structures, and eventually disrupts due to a 2,1 mode caused by re-connection between large islands located at q=2 and q=1.2-1.4, identified from soft X-ray camera measurements. Later heating leads to H-mode edge transition which prevents formation of the ITB. However, the H-mode can be delayed by interrupting the current ramp to allow the current to diffuse for about 0.5 to 1s before applying high power heating when the current ramp is resumed. This technique produces a phase with larger radius ITB + L-mode edge followed by ITB + H-mode edge about 0.5s later [Figure 9(b)]. The H-mode phase is generally ELMy, but can also exhibit short ELM-free periods. The ITB + H-mode regime is not always but usually terminated by a giant ELM rather than by core MHD activity. For ITB formation there appears to be a power threshold of about 17MW although it is possible to step-down the power during an ITB phase below the formation threshold; in these power step-down cases core MHD is observed to develop which is different to the high frequency modes which cause disruptive termination; the modes have n=1 character but are slowly rotating, located close to the q=2 surface, and degrade the confinement. The q-profile has

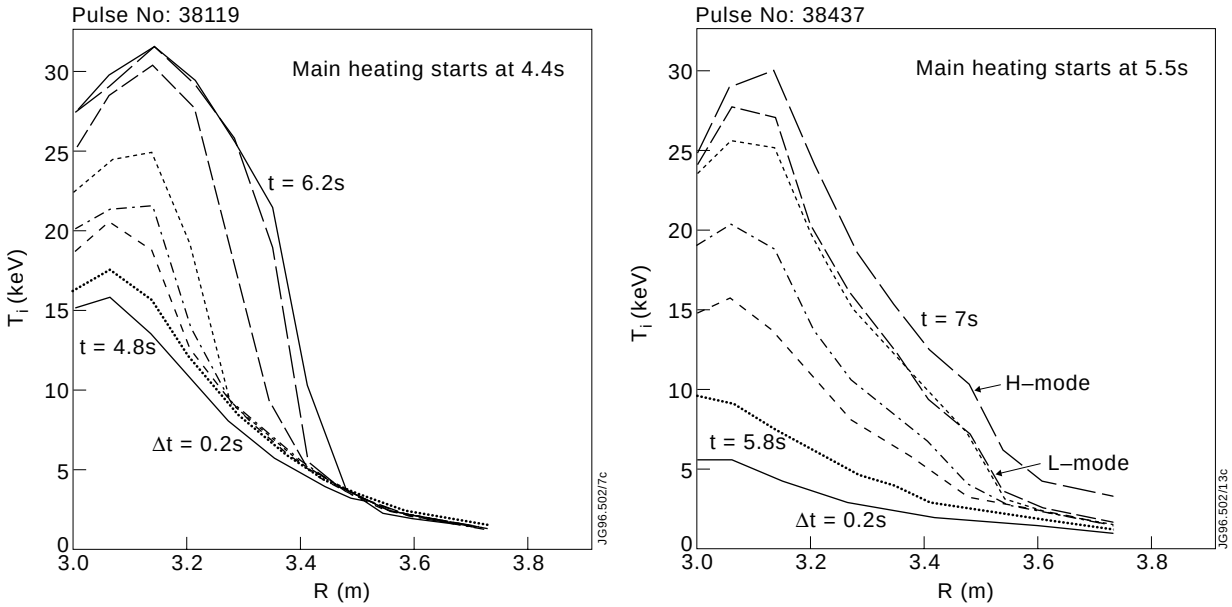

Figure 9: (a) Evolution of ion temperature profile from charge exchange recombination spectroscopy (B_T = 3.4T; 2.5 < I_p < 3MA) with early power waveform and 1MW (ICRH) pre-heating and (b) with late power application and no pre-heat

been inferred from equilibrium reconstruction under the constraint of a single polarimetry channel and the results suggest that, within the uncertainty of this reconstruction procedure, reversed shear is not necessary for ITB formation; broad current profiles and weak shear appear to be sufficient. The pressure gradient at the ITB location is very steep, as shown in Figure 10, and the shape of the pressure profile is very similar to that of the toroidal plasma rotation. However, there is evidence that NB-induced rotation is not needed for ITB formation, nor the presence of a strong central particle source, since the ITB has been established with low power NB heating by substituting higher power ICRH.

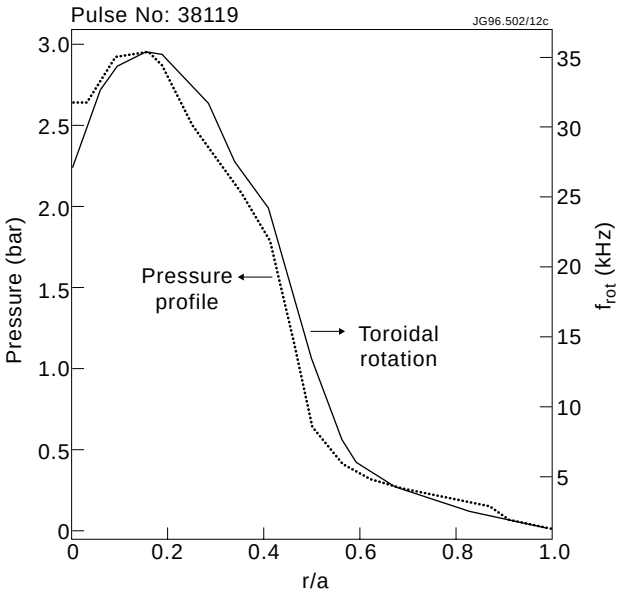

Figure 10: Profile of thermal plasma pressure and toroidal rotation profile in presence of internal transport barrier

C. High fusion performance discharges with ITB

The highest neutron rates in this regime are obtained in the combined ITB + H-mode. Figure 11 shows the time evolution of a discharge which achieved a neutron rate of 3.5×10^{16} s^{-1} for 25MW total heating power. The neutron rate and stored energy remain approximately constant over a period which exceeds an energy confinement time (0.4s). The D-D neutron rate is similar

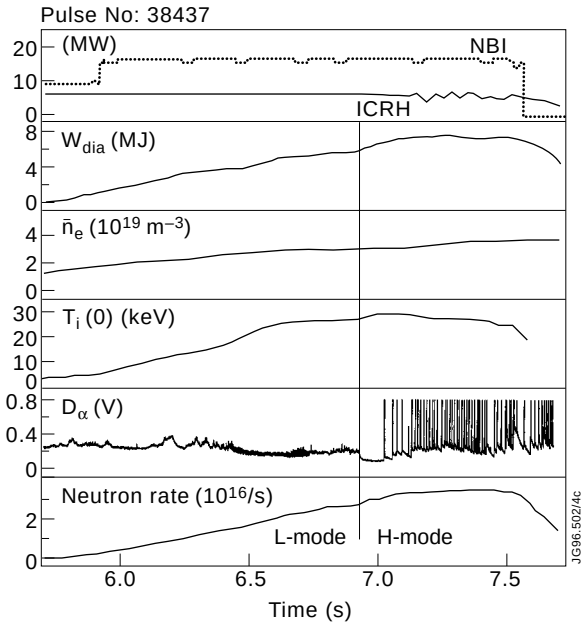

Figure 11: Time evolution of a high fusion yield pulse with shear optimisation (B_T = 3.4T; 2.5 < I_p < 3MA) with central H-minority ICRH and high power NB injection

to the best MKIIA hot-ion H-modes, but as there is no large derivative of the stored energy the loss power is much higher. Particular features of this regime are the very high central ion temperatures (≈30keV) and simultaneous high electron temperatures (15keV). The neutron rate per MJ stored energy is higher than a typical hot-ion H-mode, due to more peaked profiles; this difference means it is not possible to make a straightforward comparison of fusion triple product $n_D(0)\tau_E T_i(0)$ between the two regimes since the relationship between triple product and Q_{DT}(equiv) depends on the ion pressure profile shapes. There is no evidence of impurity accumulation within the ITB, typical values of average $Z_{eff} \approx 1.6$ having been observed. The role of ICRH (H-minority scheme) in the high performance ITB + H-mode regime is quite similar to that in the hot-ion ELM-free H-mode, discussed in section II E; due to the particularly high thermal ion β in the centre, there is significant direct ion heating. Good agreement is obtained between the measured neutron flux and computations based on plasma profile measurements using the TRANSP and PION codes. As in the case of the hot-ion H-mode, the ion heating could be further optimised for D-T performance by using multiple frequencies to reduce tail formation.

IV. ELMY H-MODE IN ITER-LIKE CONFIGURATION

A. Steady-state fusion performance

Steady-state ELMy H-modes have been obtained in large volume, moderately shaped configurations whose geometrical parameters are similar to those of ITER. Steady-state fusion yields and core plasma parameters approaching reactor-like values have been demonstrated in the MkIIA divertor, as shown by the discharge in Figure 12. To be particularly noted are the stationary values of neutron emission and $n_D(0)\tau_E T_i(0)$ in the range $4\text{-}5 \times 10^{20}$ keV.m^{-3}.s , with good particle control by the divertor leading to constant density and purity being maintained. The discharge in Figure 12 achieves 0.8 × ITERH93-P ELM-free scaling at q_{95} = 2.5 and the scaled thermal energy confinement time would therefore be within the margin required by ITER[2].

B. Current and q dependence of ELMy H-mode confinement

The confinement in long duration H-mode phases lasting many confinement times has been investigated systematically as a function of q and plasma current, including high current and power cases, at the ITER relevant values of q_{95} in the range 2.3 to 3.5. These discharges, which avoided the use of gas fuelling, typically achieved 50% of the Greenwald limit. The confinement results, normalised to ITERH93-P, are summarised in Figure 13. They indicate that the ITER confinement requirement is generally met at $q_{95} > 2.6$, including high current discharges at 4MA. There does, however, appear to be some degradation at $q_{95} < 2.6$, which is associated with the appearance of large amplitude n=2 mode activity; this activity is a property of the low q regime, as distinct from an effect of high current operation, since it affects the low current discharges as well. The deleterious n=2 activity is not always observed; in similar experiments with the MkI divertor such events were observed only rarely and therefore the problem is not considered to be fundamental although it might point to the need to avoid particular ranges of low edge q values.

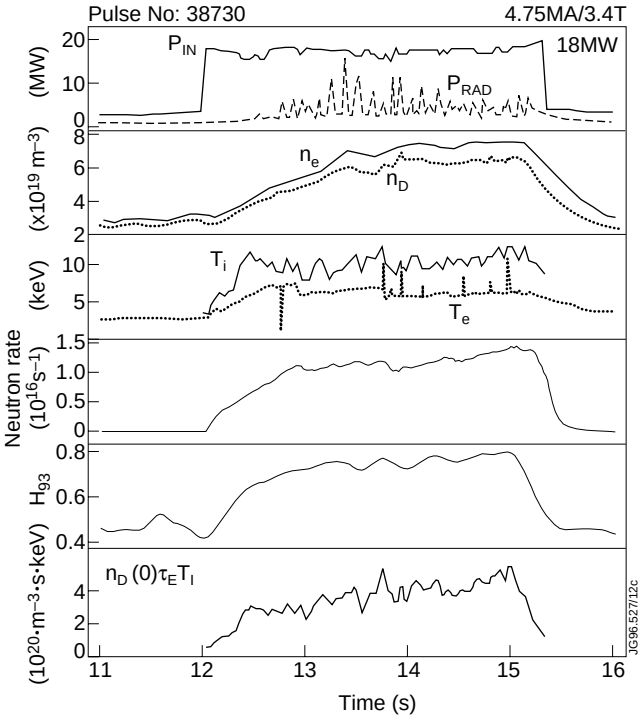

Figure 12: Time evolution of a steady-state ELMy H-mode at high current at $q_{95} \approx 2.5$

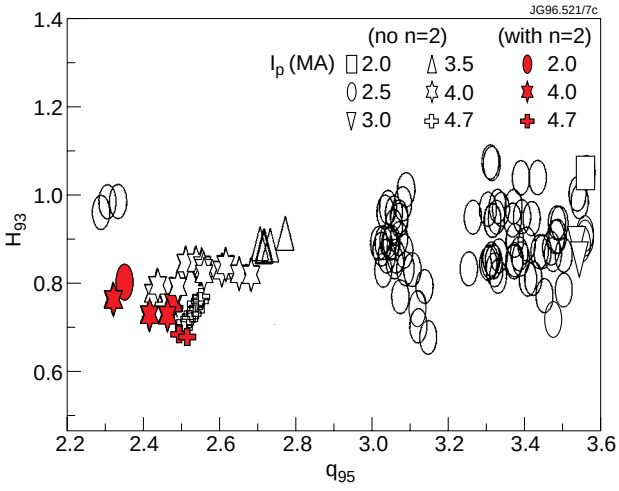

Figure 13: Normalised confinement time relative to ITERH93-P scaling (H_{93}) plotted versus q_{95} for steady-state ($\tau_H > 3\tau_E$) ELMy H-modes. The solid symbols represent discharges which were affected by strong n=2 MHD mode activity

C. Dimensionless parameter scaling of ELMy H-mode

ELMy H-mode confinement has also been studied by establishing the dependence on key dimensionless parameters which relate to the fundamental transport processes at work. In

particular, normalised larmor radius ρ^* ($\propto T^{1/2}/Ba$), collisionality ν^* ($\propto nT/B^2$) and β have been varied such that ν^* and β reached their ITER values while ρ^* was varied to within a factor of 3 of the ITER value. As far as possible, the discharges were carefully designed such that the dimensionless parameter scans were orthogonal and only one parameter was varied at a time, with $3 < \rho^*/\rho^*_{ITER} < 7$, $1.0 < \nu^*/\nu^*_{ITER} < 2.8$, and $1.0 < \beta_N < 2.2$. The purpose of this approach is to elucidate, in particular, the size scaling of confinement in the ELMy H-mode from the ρ^* dependence in order to provide a firmer basis for the extrapolation to ITER. In order to satisfy the dimensionless parameter constraints the density was varied in a range which corresponds to 70%-80% of the Greenwald limit in these experiments. The results of the study are shown in Figure 14 by comparing the experimental variation of $B\tau_E$ with that predicted form ITERH93-P scaling law which can be re-written in terms of the dimensionless parameters as follows:

$$B\tau_E(\text{ITERH93-P}) \propto \rho^{*-2.7}.\ \nu^{*-0.28}.\ \beta^{-1.2} \qquad (4)$$

The experimental data of Figure 14 support the ρ^* and ν^* dependence of ITERH93-P but $B\tau_E$ appears to have a very weak β dependence in contrast to the β degradation implied by the scaling law. This can be considered as a favourable result for ITER. The ρ^* dependence implies that the dominant transport process is close to gyro-Bohm in nature, since the latter implies a ρ^{*-3} scaling. The ELMy H-mode discharges in these experiments had low radiating fractions; in N_2 gas-seeded ELMy H-modes the confinement degraded at high radiating fractions and no longer followed gyro-Bohm ρ^* dependence and this result indicates the need for further development in this area[3,21].

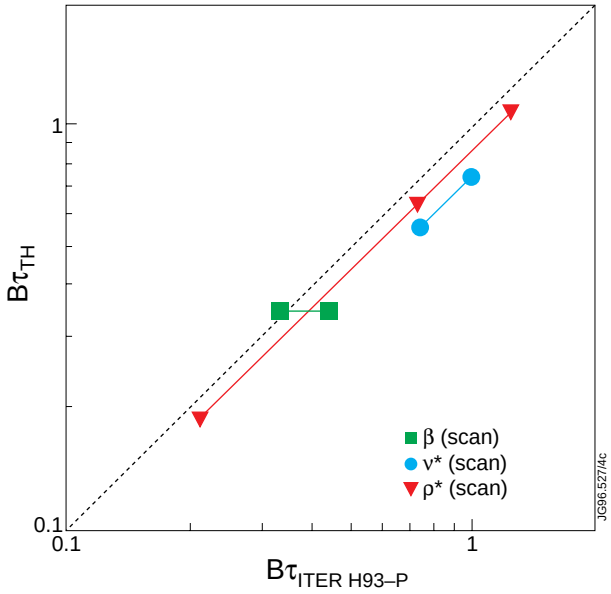

Figure 14: Normalised confinement time, expressed as $B\tau_E$, plotted versus $B\tau_{ITERH93\text{-}P}$. Three scans of ρ^* are shown as solid triangles, squares and circles. A scan of β is indicated by crosses and a υ^* scan by diagonal crosses

V. SUMMARY OF CANDIDATE SCENARIOS FOR D-T OPERATION

In order to satisfy the performance objectives of DTE1 scenarios with high D-T fusion power production are required in which the electron power balance is changed sufficiently by α-particle heating to facilitate detection. The ELM-free hot-ion H-mode is, at present, the most extensively investigated regime for maximum fusion power production in JET. At up to 17MW NB heating power the D-D fusion performance in the MkIIA divertor is very similar to that obtained previously in the MkI configuration at the same NB power. Therefore, when full NB power is available it is

expected that similar performance to the best results from the MkI campaign will be obtained. D-T projections[8] based on the best MkI discharge indicated that ≥ 10MW D-T fusion power should be achieved under the assumption that the target plasma deuteron content is replaced by 50:50 D:T and the 140kV deuterium beams from one of the two NB injector systems are replaced by tritium beams at the same power and voltage. On the basis of a simple transient definition of fusion amplification factor Q in which the absorbed additional heating power (P_{abs}) minus the rate of change of plasma stored energy (dW/dt) appears in the denominator of the term for the thermal fusion power, the best MkI campaign discharge translates to $Q_{DT}(equiv) \approx 1$ even without correcting for the α-particle heating contribution itself. This means that $P_{fus} > 10MW$ is predicted for $P_{abs} = 16MW$ and $dW/dt = 8MW$. In cases where the input power was stepped down to the loss power quasi-steady conditions[8] lasting for 1s were achieved in which $Q_{DT}(equiv) > 0.8$ would be maintained on the above definition ($P_{fus} > 6MW$ for $P_{abs} = 8MW$ and $dW/dt \approx 1MW$). It is arguable that quasi-steady conditions will be most favourable for detecting α-heating since the auxiliary heating contribution to the electron power balance will be minimised whilst high confinement is maintained, in contrast to power switch-off experiments where the heating is turned off completely. These $Q_{DT}(equiv)$ projections can be regarded as pessimistic since the NB power will be increased by 4MW to 24MW when the 140kV injector is operated in tritium, and the D-D neutron yield shows a P_{NB}^2 dependence. In addition, supplementary ICRH has now become established as a reliable method for further increasing the neutron yield, and analysis of the D-D results indicates that a significant part of the improvement is thermonuclear in origin. The ITB + H-mode with optimised current profile is established as a competitive alternative candidate for maximum fusion performance in D-T, but to date there is less operational experience. More development, including further optimisation of the current rise and heating waveforms, use of non-inductive current drive (LHCD + phased ICRH), and optimisation of the H-mode through plasma shaping are all foreseen as potential methods to increase the performance and duration of the enhanced confinement phase. Finally, in D-T the ITER-like ELMy H-modes will allow a high fusion power demonstration and provide direct experimental information on the isotope dependence of ELMy H-mode confinement and power threshold. Systematic dimensionless parameter scans similar to those described are also foreseen in 50:50 and tritium-rich plasmas in order to assess the explicit mass dependence which is needed for reliable extrapolation to ITER operation.

VI. ACKNOWLEDGEMENTS

The JET Team wishes to acknowledge the collaborations with the European Institutions which were essential to the progress made throughout this research. The optimised shear experiments reported here were conducted in collaboration with the DIII-D Team (General Atomics, USA).

VII. REFERENCES

[1] The JET Team (presented by P-H Rebut), Plasma Physics and Controlled Fusion Research (Proceedings of 13th International Conference, Washington, 1990) (International Atomic Energy Agency, Vienna) 1 **27** (1991)

[2] ITER-JCT and Home Teams (presented by G Janeschitz), Plasma Physics and Controlled Fusion **37** A19 (1995)

[3] The JET Team (presented by J Jacquinot), *Features of JET plasma behaviour in two different divertor configurations*, to be published, Plasma Physics and Controlled Fusion Research (Proceedings of 16th International Conference, Montreal, 1996) (International Atomic Energy Agency, Vienna)

[4] The JET Team, Nuclear Fusion **32** 187 (1992)

[5] B J D Tubbing, B Balet, D V Bartlett, C D Challis, S Corti, R D Gill, C Gormezano, C W Gowers, M von Hellermann, M Hugon, J J Jacquinot, H Jaeckel, P Kupschus, K D Lawson, H Morsi, J O'Rourke, D Pasini, F G Rimini, G Sadler, G L Schmidt, D F H Start, P M Stubberfield, A Tanga and F Tibone, Nuclear Fusion **31** 839 (1991)

[6] ITER H-mode Database Working Group, Proceedings of the 20th European Conference on Controlled Fusion and Plasma Physics, Lisbon (1993) (European Physical Society, Geneva) **17C Part I** 15

[7] The JET Team (presented by P J Lomas) Plasma Physics and Controlled Fusion Research (Proceedings of 13th International Conference, Seville, 1994) (International Atomic Energy Agency, Vienna) **1** 211 (1996)

[8] The JET Team (presented by T T C Jones), Plasma Physics and Controlled Fusion **37** A359 (1995)

[9] E Thompson, H P L de Esch and D Stork, Physics of Fluids **B7** 2468 (1993)

[10] R W T Koenig, K D Lawson, P J Lomas, A C Maas, P Andrew, P Breger, S Davies, A Fasoli, C Gowers, K Guenther, H Guo, J C M de Haas, T T C Jones, H Kubo, K McCormick, F B Marcus, M F Stamp, P R Thomas and K-D Zastrow, Bull. Am. Phys. Soc. **41** 1520 (1996)

[11] M F F Nave, P Smeulders, S Ali-Arshad, B Alper, P Bak, B Balet, J P Christiansen, S Clement, H P L de Esch, N Hawkes, T C Hender, G T A Huysmans, T T C Jones, R Koenig, K D Lawson, J Lingertat, P J Lomas, A Maas, F B Marcus, D P O'Brien, A Rookes, R Sartori, M F Stamp, B Schunke, P R Thomas, K Thomsen and J A Wesson, *An overview of MHD activity at the termination of JET hot-ion H-modes*, JET Report JET-P(96)14 and submitted for publication in Nuclear Fusion

[12] The JET Team (presented by A Taroni), *Energy and particle transport modelling with a time dependent combined core and edge transport code*, to be published, Plasma Physics and Controlled Fusion Research (Proceedings of 16th International Conference, Montreal, 1996) (International Atomic Energy Agency, Vienna)

[13] D Boucher and P-H Rebut, Proceedings of International Atomic Energy Agency Technical Committee Meeting on Advanced Simulations and Modelling of Thermonuclear Plasmas, Montreal (1992) (International Atomic Energy Agency, Vienna) 142 (1993)

[14] R Simonini, G Corrigan, G Radford, J Spence and A Taroni, Contributions to Plasma Physics **34** (1994) 368

[15] A Cherubini, M Erba, V V Parail, E Springmann and A Taroni, Plasma Physics and Controlled Fusion **38** 1421 (1996)

[16] G Eriksson, T E Hellsten and U Willen, Nuclear Fusion **33** 1037 (1993)

[17] C D Challis, T C Hender, J O'Rourke, S Ali-Arshad, B Alper, H J de Blank, N Deliyanakis, C G Gimblett, J Han, J Jacquinot, G J Kramer, W Kerner, D P O'Brien, P Smeulders, M F Stamp, D Stork, P M Stubberfield, D D R Summers, F Tibone, B J D Tubbing and W Zwingmann, Nuclear Fusion **31** 839 (1991)

[18] A Ekedahl, Y Baranov, J A Dobbing, B Fischer, C Gormezano, M Lennholm, V Pericoli-Ridolfini, F G Rimini, J Romero, P Schild and F X Söldner, *Profile control in JET with off-axis lower hybrid current drive*, Proceedings of 23rd European Conference on Controlled Fusion and Plasma Physics, Kiev (1996) (European Physical Society, Geneva) and submitted for publication in Plasma Physics and Controlled Fusion

[19] F M Levinton, M C Zarnstorff, S H Batha, M Bell, R E Bell, R V Budny, C Bush, Z Chang, E Frederickson, A Janos, J Manickam, A Ramsey, S A Sabbagh, G L Schmidt, E J Synakowski and G Taylor, Physical Review Letters **75** 4417 (1995)

[20] E J Strait, L L Lao, M E Mauel, B W Rice, T S Taylor, K H Burrell, M S Chu, E A Lazarus, T H Osbourne, S J Thompson and A D Turnbull, Physical Review Letters **75** 4421 (1995)

[21] The JET Team (presented by D Stork), *Optimisation of JET steady-state ELMy discharges*, to be published, Plasma Physics and Controlled Fusion Research (Proceedings of 16th International Conference, Montreal, 1996) (International Atomic Energy Agency, Vienna)

THE JET TEAM

JET Joint Undertaking, Abingdon, Oxon, OX14 3EA, U.K.

J.M. Adams[1], P. Ageladarakis, S.Ali-Arshad, B. Alper, H. Altmann, P. Andrew, N. Bainbridge, P. Bak[12], B.Balet, Y. Baranov[8], P. Barker, R. Barnsley[2], M. Baronian, K. Barth, D.V. Bartlett, A.C. Bell, E. Bertolini, V. Bhatnagar, A.J. Bickley, H. Bindslev, K. Blackler, D. Bond, T. Bonicelli, D. Borba, M. Brandon, P. Breger, H. Brelen, P. Brennan, W.J. Brewerton, M.L. Browne, T. Budd, A. Burt, P. Burton, T. Businaro, M. Buzio, C. Caldwell-Nichols, D.J. Campbell, D. Campling, P. Card, G. Celentano, C.D. Challis, A.V. Chankin, A. Cherubini, D. Chiron, J. Christiansen, P. Chuilon, D. Ciric, R. Claesen, H.E. Clarke, S. Clement, J.P. Coad, U. Cocilovo[10], I. Coffey[7], G. Conway[17], S. Cooper, J.G. Cordey, G. Corrigan, G. Cottrell, M. Cox[7], P. Crawley, R. Cusack, N. Davies, S.J. Davies, J.J. Davis, M. de Benedetti, H. de Esch, J. de Haas, E. Deksnis, N, Deliyanakis, E. di Marchi, A. Dines, S.L. Dmitrenko, J. Dobbing, N. Dolgetta, S.E. Dorling, P.G. Doyle, H. Duquenoy, A.M. Edwards[7], A.W. Edwards, J. Egedal, J. Ehrenberg, A. Ekedahl[11], T. Elevant[11], J. Ellis, M. Endler[13], S.K. Erents[7], L.G. Eriksson, H. Falter, J.W. Farthing, A. Fasoli[18], B. Fechner, M. Fichmüller, B. Fischer, G. Fishpool, C. Froger, K. Fullard, M. Gadeberg, L. Galbiati, E. Gauthier[3], R. Giannella, A. Gibson, R.D. Gill, D. Godden, A. Gondhalekar, M. Goniche[3], D. Goodall[7], C. Gormezano, C. Gowers, J. Graham, K. Guenther, R. Guirlet[3], H. Guo[22], A. Haigh, B. Haist[4], C.J. Hancock, P.J. Harbour, N.C. Hawkes[7], N.P. Hawkes[1], J.L. Hemmerich, T. Hender[7], J. Hoekzema, L. Horton, J. How, A. Howman, M. Huart, T.P. Hughes, F. Hurd, G. Huysmans, A. Hwang, C. Ibbott, C. Ingesson[15], B. Ingram, M. Irving, J. Jacquinot, H. Jaeckel, P. Jaeckel, J.F. Jaeger, O.N. Jarvis, F. Jensen, M. Johnson, E.M. Jones, L.P.D.F. Jones, T.T.C. Jones, J-F. Junger, F. Junique, A. Kaye, B.E. Keen, M. Keilhacker, W. Kerner, N.G. Kidd, Q.A. King, S. Knipe, R. Konig, J.G. Krom, H. Kubo[19], P. Kupschus, P. Lamalle[14], R. Lässer, J.R. Last, L. Lauro-Taroni, K. Lawson[7], M. Lennholm, J. Lingertat, A. Loarte, P.J. Lomas, M. Loughlin, T. Lovegrove, C. Lowry, A.C. Maas[15], B. Macklin, C.F. Maggi[16], M. Mantsinen[5], V. Marchese, F. Marcus, J. Mart, D. Martin, T. Martin, G. Matthews, H. McBryan, G. McCormick[13], G. McCracken, P.A. McCullen, A. Meigs, P. Miele, F. Milani, J. Mills, R. Mohanti, R. Monk, P. Morgan, D. Muir, G. Murphy, F. Nave[21], G. Newbert, P. Nielsen, P. Noll, W. Obert, D. O'Brien, E. Oord, R. Ostrom, M. Ottaviani, S. Papastergiou, V.V. Parail, R. Parkinson, W. Parsons, B. Patel, A. Paynter, A. Peacock, N. Peacock[7], R.J.H. Pearce, C. Perry, M.A. Pick, J. Plancoulaine, O. Pogutse, L. Porte, R. Prentice, S. Puppin, G. Radford[9], T. Raimondi, R. Reichle, V. Riccardo, E. Righi, F. Rimini, A. Rolfe, A. Rookes[12], R.T. Ross, A. Rossi, L. Rossi, G. Sadler, G. Saibene, M. Salisbury[12], A. Santagiustina, F. Sartori, R. Sartori, R. Saunders, P. Schild, M. Schmid, V. Schmidt, B. Schokker[15], B. Schunke, M. Scibile, S.M. Scott, S. Sharapov, A. Sibley, R. Simonini, A.C.C. Sips, P. Smeulders, O. Smith[12], P. Smith, R. Smith, F. Söldner, J. Spence, E. Springmann, M. Stamp, P. Stangeby[20], D.F. Start, D. Stork, P.E. Stott, P. Stubberfield, D. Summers, L. Svensson, P. Svensson, A. Tabasso[12], M. Tabellini, J. Tait, A. Tanga, A. Taroni, C. Terella, P.R. Thomas, K. Thomsen, B. Tubbing, Y. Ul'Haq[12], A. Vadgama, P. van Belle, R. van der Linden, G. Vlases, M. von Hellermann, T. Wade, R. Walton, D. Ward, M.L. Watkins, N. Watkins[1], M.J. Watson, J. Wesson, M. Wheatley, D. Wilson, T. Winkel, C. Woodward, D. Young, I.D. Young, Q. Yu[6], F. Zannelli, K-D. Zastrow, W. Zhang[12], N. Zornig, W. Zwingmann.

PERMANENT ADDRESSES

1. UKAEA, Harwell, Didcot, Oxon, UK.
2. University of Leicester, Leicester, UK.
3. CEA, Cadarache, France.
4. KFA, Jülich, Germany.
5. Helsinki University of Technology, Espoo, Finland.
6. Institute of Plasma Physics, Hefei, P R of China.
7. UKAEA Culham Laboratory, Abingdon, Oxon, UK.
8. A.F. Ioffe Institute, St. Petersburg, Russia.
9. Institute of Mathematics, University of Oxford, UK.
10. ENEA, CRE Frascati, Roma, Italy.
11. Royal Institute of Technology, Stockholm, Sweden.
12. Imperial College, University of London, UK.
13. Max Planck Institut für Plasmaphysik, Garching, Germany.
14. Plasma Physics Laboratory, ERM-KMS, Brussels, Belgium.
15. FOM Instituut voor Plasmafysica, Nieuwegein, The Netherlands.
16. Dipartimento di Fisica, University of Milan, Milano, Italy.
17. University of Saskatchewan, Saskatoon, Canada.
18. EPFL, Lausanne, Switzerland.
19. JAERI, Tokyo, Japan.
20. Institute for Aerospace Studies, University of Toronto, Canada.
21. LNETI, Savacem, Portugal.
22. INRS-Energieet Materiaux, Univ. du Quebec, Canada.